CD AND FLUORESCENCE SPECTROSCOPIC PROPERTIES OF THE MAJOR CORE PROTEIN OF FELINE IMMUNODEFICIENCY VIRUS AND ITS TRYPTOPHAN MUTANTS.

Assignment of the individual contribution of the aromatic side chains

Running title: CD and fluorescence of FIV-rp24 and Trp mutants

Belén Yélamos[1], Elena Núñez[1], Julián Gómez-Gutiérrez[1], Manisha Datta[2], Beatriz Pacheco[1], Darrell L. Peterson[2] and Francisco Gavilanes[1]

[1]Departamento de Bioquímica y Biología Molecular I. Facultad de Ciencias Químicas. Universidad Complutense de Madrid. 28040 Madrid, Spain.

[2]Department of Biochemistry and Molecular Biophysics. Virginia Commonwealth University. Richmond. 23298 Virginia, USA.

Subdivision: Protein chemistry and structure

Corresponding to F. Gavilanes, Departamento de Bioquímica y Biología Molecular I. Facultad de Ciencias Químicas. Universidad Complutense de Madrid. 28040 Madrid, Spain. Fax: + 34 91 394 4159. Tel.: + 34 91 394 4266

E-mail: pacog@solea.quim.ucm.es

ABBREVIATIONS

CCA, convex constraint analysis; EIAV, equine infectious anemia virus; FIV, feline immunodeficiency virus; FIV-rp24, recombinant FIV p24 protein; HIV, human immunodeficiency virus; NTA, nitrilotriacetic acid; SIV, simian immunodeficiency virus; W40F, recombinant p24 protein with Phe at position 40 instead of Trp; W126F, recombinant p24 protein with Phe at position 126 instead of Trp; W40/126F, recombinant p24 protein with Phe at positions 40 and 126 instead of Trp.

SUMMARY

The gene coding for the major capsid protein of feline immunodeficiency virus (FIV) has been cloned into the expression vector pQE60 which allows protein purification by affinity chromatography on a Ni-Nitrilotriacetic-Agarose column. The gene was expressed in *Escherichia coli* and the resultant soluble protein (FIV-rp24) purified to electrophoretic homogeneity. The amino acid composition of the recombinant protein is practically coincident with that predicted from the DNA sequence. This protein has two tryptophan residues at positions 40 and 126 that have been replaced by phenylalanine by site directed mutagenesis to obtain two single mutants and a double mutant. Circular dichroism and fluorescence spectroscopy were employed to study the structural features of FIV-rp24 protein and its tryptophan mutants. The analysis of the CD spectra indicated that α-helix is the major secondary structure element (48-52%) and that the overall three-dimensional structure is not modified by the mutations. The fluorescence emission spectra pointed out that both Trp residues occupy a highly hydrophobic environment. Moreover, the different Tyr fluorescence intensities of wild type and mutant proteins are indicative of the existence of resonance energy transfer processes to nearby Trp. The individual contributions of each tryptophan residue to the spectroscopic properties of the wild type protein were obtained from the spectra of all these proteins. Thermal denaturation studies indicate that both tryptophan residues do not contribute equally to the stabilization of the three-dimensional structure.

Keywords: FIV core protein; tryptophan mutants; site-directed mutagenesis; circular

dichroism; fluorescence spectroscopy.

INTRODUCTION

Lentiviruses are a subfamily of retroviruses to which belong, among others, feline immunodeficiency virus (FIV), equine infectious anemia virus (EIAV), simian immunodeficiency virus (SIV) and human immunodeficiency virus (HIV), the etiological agent of acquired immunodeficiency syndrome. The biological and genetic relationships between the non-human lentiviruses and HIV-1 render them potentially useful models for understanding the pathogenesis of HIV-1, and for evaluating methods of effective treatment and control of viral infection [1].

FIV, a common pathogen in both domestic and wild cats worldwide, was first isolated in 1986 from specific pathogen-free kittens inoculated with peripheral blood or plasma from a cat with an acquired immunodeficiency syndrome-like disease in the United States [2, 3]. FIV was then classified as a lentivirus on the basis of virion morphology, Mg^{2+}-dependent reverse transcriptase activity, and the propensity for persistent infection in cats [2, 3]. This lentivirus causes generalized lymphoadenopathy and increased susceptibility to opportunistic infections, eventually culminating in death [4].

Members of the lentiviruses share many common features, including a large RNA genome of 9 kb or more in length, and exhibit conserved genomic organization [5]. The *Gag* (or core) open reading frame is located at the 5' end of the genome, immediately following the 5' long terminal repeat, and is the first gene to be translated [5]. Consistent with other lentiviruses, proteolytic processing sites within the Gag polyproteins of FIV were identified [6]. The precursor protein of Gag is processed to yield different proteins: p15 (matrix protein), p24 (capsid protein), p7 (nucleocapsid

protein) and p6 [6, 7].

An alignment of lentiviral gag amino acid sequences indicates that the region of highest identity includes the major core protein and the nucleocapsid protein. Pairwise comparisons of FIV to other lentiviruses reveal important amino acid identities with EIAV (49%), visna virus (43%), and HIV-1 (40%) [8, 9]. Indeed, serological cross-reactivity to the capsid protein was demonstrated among FIV, visna virus and EIAV [10, 11]. This is indicative of the presence of conserved interspecies determinants among the lentiviral core proteins, prompting suggestion that the major core proteins of at least HIV-1, FIV, and EIAV are organized into similar antigenic domains.

Moreover, the high degree of amino acid similarity combined with immunological cross-reactivities and conserved function, suggest that the three-dimensional structure of the lentiviral core proteins are likely to be related. In fact, the core proteins of EIAV and HIV have been shown to possess the same overall three-dimensional structure being organized into two domains linked by a flexible extended peptide [12-16]. The N-terminal domain has a compact bullet shape composed of five coiled-coil α-helices, with two additional short α-helices following an extended proline-rich loop [12, 13]. The C-terminal domain has four bundled α-helices and an extended strand [14]. The EIAV protein crystallizes as dimers with head-to-head interactions [15] while the dimers observed in crystals of HIV capsid protein complexed with a monoclonal antibody Fab have head-to-tail interactions [16].

In this study we report the cloning, expression and purification of the major core protein of FIV. The recombinant protein has two tryptophan residues at positions

40 and 126, which have been replaced by one or two phenylalanine residues to obtain two single mutants and one double mutant. The CD and fluorescence properties of the wild type and mutant proteins have been determined. From them, the individual contribution of the aromatic side chains have been resolved.

EXPERIMENTAL PROCEDURES

Materials

Restriction enzymes, polymerases and other molecular biology reagents were obtained from New England Biolabs and Qiagen. CL-6B Ni-NTA agarose was purchased from Qiagen. All other reagents were from Merck.

Cloning strategy

The gene that codes for the major core protein of FIV was amplified by a standard PCR reaction using Vent polymerase (New England Biolabs). The following conditions were employed: 5 cycles at 94 °C, 42 °C and 72 °C, each for 1 min; followed by 25 cycles at 94 °C, 55 °C and 72 °C, each for 1 min. A final 'filling-in' step at 72 °C for 5 min was incorporated to assure that the ends of the PCR reaction were 'flush'. The product of the PCR reaction was run on an agarose gel (0.8%), and a 699 bp product was extracted using the 'Qiaex' DNA extraction kit (Qiagen). The primers used for the PCR were:

p24-NcoI(+): GCCCATGGTACCTATTCAAACAGTA

p24-BglII(-): GGAGATCTAAGAGCTTCTGCCAAGAG

They were designed in such a way that the product had an *Nco*I restriction site (CCATGG) at its 5' end and a *Bgl*II restriction site (AGATCT) at its 3' end. The 699 bp DNA fragment was doubly digested by the restriction enzymes *Nco*I and *Bgl*II and cloned into the expression vector pQE60 (Qiagen) which had been cleaved

with the same two enzymes to obtain the plasmid pQE60-FIV/p24. pQE60 is an expression vector that adds a six histidines sequence at the carboxyl-terminal end of the protein. The initiator Met residue is coded by the triplet ATG within the *Nco*I restriction site. The ligation was carried out by incubating 50 ng of both plasmid and insert and 200 units of T4-DNA-ligase (New England Biolabs) in a total volume of 20 μl for 15 h at 16 °C. A positive clone was identified by restriction analysis of mini-prep DNA and ultimately by automated sequencing which was performed by the Universidad Complutense DNA sequencing Facility by using an ABI Prism 377 system.

Preparation of tryptophan mutants of FIV major core protein

The tryptophan mutants were obtained using the PCR technique and the plasmid pQE60-FIV/p24 as template. The primers used to generate the mutations were:

W40F(+): CAATTGTTCTTTACTGCCTTCTCTGCA

W40F(-): GGTGAGGAAGTTCAATTGTGGTTT

W126F(+): TGGTATCTAGAGGCATTAGGA

W126F(-): AGGATGCAGTGTAGAGCATTTTATCTAGAG

These primers have specific changes of bases corresponding to the mutation and they incorporate new restriction sites, *Mfe*I (CAATTG) in the W40F mutant, and *Xba*I (TCTAGA) in the W126F mutant. The PCR reactions were carried out employing the following conditions: 5 cycles at 94 °C (30 s), 37 °C (12 s), 72 °C (20 s); followed by 30 cycles at 94 °C (30 s), 55 °C (12 s), 72 °C (20 s) and a final step at

72 °C (7 min). For each mutant two PCR reactions were carried out. Thus, for W40F mutant p24-NcoI(+)/W40F(-) and W40F(+)/p24-BglII(-) primer pairs were used. The two fragments obtained were digested with the restriction enzymes, *Mfe*I (W40F) or *Xba*I (W126F), and ligated. The DNA fragments that encoded the W40F and W126F mutants, generated by ligation, were amplified by a second PCR reaction, digested with the restriction enzymes *Nco*I and *Bgl*II and cloned into the expression vector pQE60 cleaved with the same restriction enzymes to obtain the plasmids pQE60-W40F and pQE60-W126F. The following strategy was employed to obtain the double mutant: pQE60-W40F plasmid was digested with the restriction enzymes *Nco*I and *Hind*III to get a 216 bp fragment, and pQE60-W126F plasmid was digested with *Hind*III and *Bgl*II to get a 473 bp fragment. These fragments were ligated to the pQE60-FIV/p24 plasmid digested with the restriction enzymes *Nco*I and *Bgl*II. The changes introduced were confirmed by digestion of the pQE60-W40F and pQE60-W126F plasmids with the restriction enzymes *Mfe*I or *Xba*I respectively, and by automated DNA sequencing.

Expression and purification of FIV core protein and tryptophan mutants

E. coli strain M15[pREP4] was transformed with pQE60-FIV/p24 plasmid by the $CaCl_2$ method [17] and plated onto a LB (Luria-Bertani) plate supplemented with 100 μg/ml ampicillin and 25 μg/ml kanamycin. These cells have multiple copies of the pREP4 plasmid, which has the *lac*I gene [18], that encodes the *lac* repressor and gives kanamycin resistance to the cell. A single colony was selected and used to inoculate 100 ml of LB media supplemented with 100 μg/ml ampicillin and 25 μg/ml

kanamycin. This culture was grown overnight at 37 °C and then used to inoculate 2 L of the same media which were grown until A_{600} reached a value of 0.5-0.6. The expression of the protein was induced by 0.25 mM IPTG for 4 h at 37 °C. The cells were harvested by centrifugation at 6000 rpm for 10 min. Cell pellets were resuspended in 10 mM Tris, pH 8.0 (30 ml/L of cell culture) and lysed by sonication. The cell lysate was clarified by centrifugation at 89500 *g* for 30 min in a Beckman SW28 rotor. The supernatant was supplemented with 10 mM Imidazole and loaded onto a Sepharose CL-6B Ni-NTA column which had previously been equilibrated with 10 mM Tris, 10 mM Imidazole, pH 8.0. Once the protein solution had entered the column, it was washed with 5 column volumes of 10 mM Tris, 10 mM Imidazole, pH 8.0 and later with 10 mM Tris, 30 mM Imidazole, pH 8.0. The recombinant FIV-p24 protein (FIV-rp24) was eluted with 10 mM Tris, 200 mM Imidazole, pH 8.0. The presence of FIV-rp24 was monitored by SDS-PAGE throughout the purification. The same protocol was used to purify the mutant proteins.

SDS-PAGE

Analytical polyacrylamide gel electrophoresis was performed according to the method of O'Farrell [19]. 4% acrylamide stacking gel and 15% acrylamide resolving gel were employed. Gels were stained with Coomassie brilliant blue R-250.

Amino acid analysis

Approximately, 20 μg of purified protein were hydrolyzed with 5.9 N

hydrochloric acid, 0.1% (w/v) phenol, at 115 °C for 24 h. The amino acid analysis was performed on a Beckman 6300 automatic analyzer.

Circular dichroism measurements

Circular dichroism spectra were obtained on a Jasco J-715 spectropolarimeter using 0.1 cm or 1 cm pathlength cuvettes at 25 °C. The protein concentration was 0.1-0.2 mg/ml for far-UV and 1 mg/ml for near-UV. The buffer used was 10 mM sodium phosphate, pH 7.0. A minimum of four spectra were accumulated for each sample and the contribution of the buffer was always subtracted. The resultant spectra were smoothed using J715 Noise Reduction software. The values of mean residue molar ellipticity $[\Theta]_{MRW}$ were calculated on the basis of 113 as the average molecular mass per residue and they are reported in terms of degree $\cdot$ cm^2 $\cdot$ $dmol^{-1}$. The secondary structure of the protein was evaluated by computer fit of the dichroism spectra according to the algorithm Convex Constrain Analysis (CCA) [20]. This method relies on an algorithm that calculates the contribution of the secondary structure elements that give rise to the original spectral curve without referring to spectra from model systems. Thermal denaturation curves were obtained by measuring continuously the ellipticity at 208 nm over the range 25-75 °C. The temperature in the cuvette was regulated with a Neslab RT-11 circulating water bath and was increased at 30 °C/h. The T_m values were determined from the first derivative of the smoothed denaturation curves.

Fluorescence measurements

Fluorescence studies were carried out on a SLM Aminco 8000C spectrofluorimeter, fitted with a 450 W xenon arc. The protein concentration was 0.05-0.1 mg/ml. A 0.4x1 cm cuvette was used. The buffer used was 10 mM sodium phosphate, pH 7.0. The temperature in the cuvette (25 °C) was maintained by a Polystat Hubber circulating water bath. Excitation was performed at 275 or 295 nm, and the emission spectra were recorded over the range 285-450 nm. The contribution of the buffer was always subtracted. The tyrosine contribution to the emission spectra was calculated by subtracting from the emission spectra measured at λ_{exc}= 275 nm the emission spectra measured at λ_{exc}= 295 nm multiplied by a factor. The factor was obtained from the ratio between the fluorescence intensities measured with λ_{exc}= 275 and λ_{exc}= 295 nm at wavelengths higher than 380 nm, where there is no tyrosine contribution.

RESULTS

Cloning, expression and purification of FIV-rp24 and tryptophan mutants

Following the strategy described in the Experimental Procedures section (Fig. 1), the gene coding for the major core protein of FIV was cloned in the expression vector pQE60. The DNA sequence of the PCR-generated p24 clone was identical to the published sequence of the proviral DNA [9], except in the zones corresponding to the amino- and carboxyl-ends of the protein which, as explained below, have some extra amino acids. Using the plasmid pQE60-FIV/p24 as template and the corresponding primers, the W40F, W126F and W40/126F mutant genes were obtained. Their sequence was confirmed by automated sequencing and was identical to that of cloned p24 except where the triplet TGG has been changed to TTC (W40F) or TTT(W126F). Expression of either constructed gene yielded a protein with a molecular mass of 27.5 kDa. Fig. 2 shows an SDS-polyacrylamide gel of the purification steps of FIV-rp24. Similar results were obtained for the single and double mutants. The protein expressed in a soluble form was subsequently purified using affinity chromatography on a Ni-NTA-Agarose column. The protein that eluted with 200 mM imidazole was determined to be >95% pure by densitometry of stained SDS gels (Fig. 2, lane 5). Following this procedure, approximately 5 mg of FIV-rp24 protein, 4 mg of W40F mutant, 2 mg of W126F mutant and 2 mg of the double mutant were obtained from 1 L of culture media.

The amino acid sequence of the wild type recombinant protein, as deduced from the cDNA sequence, differs from the actual core protein, which is 223 amino

acids long, in the following aspects: the two additional amino acids, Met and Val, at the amino-terminus due to the introduction of the *Nco*I restriction site; an extension of four amino acids (Ala-Glu-Ala-Leu) at the carboxyl-terminus which in the precursor polyprotein are between p24 and p7 [6]; the two amino acids, Arg and Ser, at the carboxyl-terminus due to cloning into *Bgl*II pQE60 site; finally, the six histidine residues tag. Thus, the recombinant protein is 237 amino acids long and the two Trp occupy positions 40 and 126 which in the original protein correspond to positions 38 and 124, respectively. The amino acid composition of FIV-rp24 and mutant proteins are shown in Table 1. As it can be observed, the amino acid composition of the cloned protein is practically coincident with that predicted from the DNA sequence. The lower Met content of cloned proteins could be due to either the proteolytic cleavage of the initiator formyl-methionine residue, as frequently reported when proteins are expressed and purified from *E. coli* [22], or the amino acid analysis procedure used. The number of Trp residues decreased for the mutants and, accordingly, the number of Phe residues increased.

Absorption spectra of FIV-rp24 and tryptophan mutants

When analyzed by ultraviolet spectroscopy, purified FIV-rp24 protein gave an absorption spectrum characteristic of a soluble protein (Fig. 3). It exhibited a maximum at 277 nm and two shoulders at 281 and 292 nm. The shoulder at 292 nm was less evident in the single Trp mutants and almost disappeared in the double mutant. The spectrum of the double mutant was coincident with that of free tyrosine in solution although it is red-shifted, indicating that protein tyrosine residues occupy a

hydrophobic environment. The shoulders between 255-265 nm should be the contribution of the seven Phe residues. The molar extinction coefficients were determined by amino acid analysis of aliquots of protein solutions of known A_{280} and were 23120, 17110, 17365 and 11565 M^{-1} cm^{-1} for FIV-rp24, W40F, W126F and W40/126F, respectively. Therefore, a 1 mg/ml solution of these proteins was found to have an A_{280} of 0.88, 0.65, 0.67 and 0.44 respectively.

Circular dichroism spectra

The far-UV CD spectra of FIV-rp24 and its Trp mutants are depicted in Fig. 4A. All the spectra show two minima at 208 and 222 nm and a maximum at 191 nm indicatives of a high content of α-helical structure. The assignment of the secondary structure elements calculated from these spectra, according to the algorithm CCA [20] is shown in Table 2. The major component in all the proteins is α-helix (48-52%) with no β-sheet present.

The near-UV CD spectrum of FIV-rp24 is a complex mixture of multiple Cotton effects (Fig. 4B). A major negative band at 269 nm together with minor negative bands at 262, 275, 284 and 296 nm and minor positive bands at 258 and 290 nm were observed. The assignment of a particular band to a given residue could be performed by analyzing the spectra of the mutant proteins. Since the contributions of the inserted Phe residues to the near-UV CD spectrum above 260 nm is almost negligible [23], the contribution of each Trp can be obtained by difference spectra. Fig. 5 shows the individual contribution of Trp40 and Trp126 as determined either from the spectrum of wild type FIV-rp24 (FIV-rp24 - Trp mutant) or from the single

mutant spectra (Trp mutant - double mutant). Above 265 nm the results of both calculations are virtually indistinguishable. The spectrum of either Trp residue is a complex combination of bands. The contribution of Trp40 is positive in the entire wavelength range with maxima at 273, 283 and 290 nm and it should be responsible for the positive band observed at 290 nm in the wild type FIV-rp24. The Trp126 spectrum has two major negative bands centered at 272 nm and 295 nm. The former cancels the positive contribution of Trp40 at that wavelength and the later should be responsible for the negative band which in native FIV-rp24 appeared at 295 nm. The position of the different bands indicated a more hydrophobic environment of Trp126.

On the other hand, the spectrum of the double mutant revealed the important contribution of aromatic side chains other than Trp, mainly Tyr residues, to the near-UV CD spectrum of FIV-rp24 with negative bands at 262, 269, 278 and 284 nm. Addition of this spectrum to those calculated for Trp40 and Trp126 rendered the spectra depicted in Fig. 6. Except for the 250-265 nm range the composite spectrum possesses all features of the FIV-rp24 near-UV spectrum, independently of the method used to calculate the individual Trp contribution.

Fluorescence emission spectra

The fluorescence emission spectra of FIV-rp24 and its Trp mutants are depicted in Fig. 7. Upon excitation at 275 nm both FIV-rp24 and W40F mutant exhibited a maximum at 320 nm (Fig. 7A and B) which indicates that the fluorescence of these proteins is highly dominated by Trp residues and that they occupy a highly hydrophobic environment. However, the maximum of W126F appeared at 303 nm

(Fig. 7C), indicative of a high contribution of Tyr residues to the fluorescence intensity. Moreover, the two Trp should not contribute equally to the fluorescence of FIV-rp24 since at 320 nm the fluorescence intensity of W40F and W126F mutants was respectively 70% and 50% that of wild type FIV-rp24. The spectrum of W40/126F mutant provided the contribution of the seven Tyr residues to the protein fluorescence (Fig. 7D).

Upon excitation at 295 nm the position of the fluorescence emission maximum was around 321-322 nm for both wild type and single mutants but differences in fluorescence intensity were observed (Fig. 7). Thus, the value for W40F mutant was 68% that of the wild type while the value for W126F mutant was only 33%. Then, the contribution of Trp126 to the spectrum must be twice that of Trp40. Moreover, the protein fluorescence of FIV-rp24 observed upon excitation at 295 nm arises almost exclusively from tryptophan residues as indicated by the low spectrum of the double mutant (Fig. 7D), which accounts for only 7% of the fluorescence intensity of the wild type protein.

The difference between the fluorescence spectra obtained upon excitation at 275 and 295 nm, being the later normalized, provides the contribution of Tyr residues to the protein fluorescence. In the case of wild type and W40F proteins Tyr accounts for almost 40% of the intensity obtained upon excitation at 275 nm and this value increased to 75% for W126F protein. However, in none of them the intensity was even close to the authentic Tyr fluorescence given by W40/126F mutant.

Thermal stability of FIV-rp24 and Trp mutants

The thermal denaturation of either protein was followed by measuring continuously the ellipticity at 208 nm upon increasing the temperature at 30 °C/h (Fig. 8). In all cases the process was cooperative and differences on the temperature at the midpoint (T_m) were observed. Thus, wild type protein and W40F mutant had a close T_m value, 63.4 ± 0.9 °C and 61.2 ± 0.4 °C, respectively. The stability of the protein decreased when Trp126 was mutated since the T_m for W126F and double mutant was 52.3 ± 0.4 °C and 54.4 ± 0.4 °C, respectively.

DISCUSSION

Site directed mutagenesis performed on aromatic amino acids, especially tryptophans, has often been used to create proteins with intrinsic probes which can be used to monitor their unfolding, refolding, and stability [24-26]. This procedure is based on the knowledge that the spectral properties of these amino acids are highly dependent on their three-dimensional environment. On the other hand, feline immunodeficiency virus represents a valuable animal model for studying the human immunodeficiency virus [27]. As stated before the high degree of sequence homology exhibited by lentiviral core proteins [8, 9] together with immunological cross-reactivities [10, 11] would suggest a common tertiary structure. Studies of the structure and folding of this family of proteins, which have important roles in virus morphology and assembly process [28-30], may have applications in anti-viral therapy and vaccine development [31, 32]. In this report we detail the cloning, expression and spectroscopic properties of the major core protein of FIV, as well as its two single tryptophan mutants (W40F and W126F) and the double mutant (W40/126F).

The higher order structure of FIV-rp24 and its Trp mutants was studied using circular dichroism and fluorescence spectroscopy. The far-UV circular dichroism spectrum of the wild type protein is similar to that described for the capsid protein of HIV-1 [33,34] and EIAV [35], and indicates that FIV-rp24 is predominantly α-helical. The percentage of FIV-rp24 α-helix calculated from the CD spectrum is coincident with that of EIAV-p26 [15] and HIV-p24 [16] as deduced from their crystal structure. Thus, as expected from their position at the ends of the polypeptide chain, the 14

extra amino acids of the recombinant protein, including the histidine tag, seem not to alter the overall structure. However, the possibility that the extra amino acids have some local effect or modify somehow the protein stability cannot be excluded from these studies. Moreover, the substitution of one or two tryptophan residues by phenylalanine did not have any influence in the far-UV CD spectrum of the protein, indicating that the secondary structure remained unchanged after the mutation and also that the aromatic side chains do not contribute to the CD spectrum in this wavelength range as it has been reported for proteins with a low intensity CD spectrum [36].

The aromatic side chains of FIV-rp24 contribute to the near-UV CD spectrum with a complex combination of Cotton effects, all positive for Trp40, positive and negative for Trp126 and all negative for the seven Tyr residues. The inserted Phe residues could have a low contribution to the spectrum of the mutants but always below 260 nm [23]. The spectra of Trp and Tyr residues could be added to obtain a composite spectrum which, except for the 250-265 nm range, has a high resemblance with that of wild type FIV-rp24. The practical coincidence of both spectra above 265 nm indicates that substitution of any Trp causes only alterations at the point of mutation without modifying the environment of the other Trp. The non-coincidence between the experimental and calculated spectra in the aforementioned range could be due to the fact that at least the double mutation has caused some minor conformational changes around the neighbor Tyr residues which have led to spectral changes in this wavelength region. Since the composite spectra are obtained by adding to the double mutant spectrum the individual Trp contributions, they could not coincide with that of the wild type protein in the 250-265

nm region. Another plausible explanation is that small variations of protein concentration would render significant changes between the spectra, because of the high relative contribution of peptide bonds to the ellipticity values in that spectral range.

The emission fluorescence of tryptophan and tyrosine vary widely from one protein to another due to the existence of quenching and resonance energy transfer processes [37, 38]. In the case of FIV-rp24 Tyr fluorescence accounts for almost 40% of the fluorescence intensity upon excitation at 275 nm. Taking into account that there are seven Tyr residues, the average contribution of each Tyr (6%) is lower than that of each Trp (30%). The emission spectrum of W40/126F mutant gives the authentic Tyr contribution. Resonance energy transfer to nearby Trp should be responsible for the lower Tyr contribution exhibited by both wild type and single mutant proteins. Modeling of FIV-p24 structure with that described for EIAV-p26 [15] or HIV-p24 [16] indicates that Tyr to Trp energy transfer is a feasible process. Specifically, the distance from Tyr81 and Tyr127 to Trp126 and from Tyr127 to Trp40 is within that necessary for energy transfer to take place. Moreover, this fact would account for the lower Tyr contribution to the fluorescence spectrum of wild type and W40F proteins. On the other hand, the different fluorescence intensities of W40F and W126F mutants upon excitation at 295 nm pointed out a different degree of quenching of the indole ring by close side chains. As a result Trp126 contributes double than Trp40 to the fluorescence intensity of FIV-rp24. The emission spectra obtained upon excitation at 295 nm provide additional indications that the changes induced by the substitutions should be restricted to the point where the mutations take place. Thus, the position of the maximum, 321-322 nm, does not change when

Phe residues are inserted. Moreover, addition of W40F and W126F spectra provides a spectrum which is similar in shape to that of wild type protein and with a 95% of its fluorescence intensity (data not shown).

The spectroscopic properties of FIV-rp24 and single and double mutants indicate that the mutational changes introduced in the protein do not affect the overall tertiary structure. However, a difference in thermal stability of mutant proteins has been observed, indicating that the W126F and W40/126F mutants are thermally less stable than the wild type FIV-rp24 and W40F mutant. If the three-dimensional structure of lentiviral core proteins is conserved, Trp126 would occupy the “a” position of one of the heptad repeats of G helix while Trp40 would be in the heptad “g” position of B helix [12]. The former would take part in helix-helix contacts that make the bundle, a position which is more hydrophobic than that occupied by the later. Thus, Trp126 would contribute more to the stabilization of the three-dimensional structure and hence the lower thermal stability of W126F and W40/126F mutants. Anyway, the four proteins seem to be stable enough to be considered as valuable tools for the study of the folding mechanism of the protein. The assigned bands can be used as specific structural probes to follow the kinetics and the formation of folding intermediates which should help us to understand how the FIV-rp24 protein assumes its native conformation.

ACKNOWLEDGMENTS

This work was supported by Grants from the DGES (Spain) (PB96-0602) and from the NIH (USA) (AI15955).

REFERENCES

[1] Letvin, N.L. (1990) Animal models for AIDS. *Immunol. Today* **11**, 322-326.

[2] Pedersen, N.C., Ho, E.W., Brown, M.L. & Yamamoto, J.K. (1987) Isolation of a T-lymphotropic virus from domestic cats with an immunodeficiency-like syndrome. *Science* **235**, 790-793.

[3] Olmsted, R.A., Langley, R., Roelke, M.E., Goeken, R.M., Adger-Johnson, D., Goff, J.P., Albert, J.P., Packer, C., Laurenson, M.K., Caro, T.M., Scheepers,L., Wildt, D.E., Bush, M., Martenson,J.S. & O'Brien, S.J. (1992) Worldwide prevalence of lentivirus infection in wild feline species: epidemiologic and phylogenetic aspects. *J. Virol.* **66**, 6008-6018.

[4] Pedersen, N.C., Yamamoto, J.K., Ishida,T. & Hansen, H. (1989) Feline immunodeficiency virus infection. *Vet. Immunol. Immunopathol.* **21**, 111-129.

[5] Clements, J.E. & Wong-Staal, F. (1992) Molecular biology of lentiviruses. *Sem. Virol.* **3**, 137-146.

[6] Elder, J.H., Schnolzer, M., Hasselkus-Light, C.S., Henson, M., Lerner, D.A., Phillips, T.R., Wagaman, P.C. & Kent, S.B.H. (1993) Identification of proteolytic processing sites within the Gag and Pol polyproteins of feline immunodeficiency virus. *J. Virol.* **67**, 1869-1876.

[7] Steinmann, R., Dombrowski, J., O'Conner, T., Montelaro, R.C., Tonelli, Q., Lawrence, K., Seymor, C., Goodness, J., Pederson, N. & Anderson, P.R. (1990) Biochemical and immunological characterization of the major structural proteins of feline immunodeficiency virus. *J. Gen. Virol.* **71**, 701-706.

[8] Olmsted, R.A., Hisch, V.M., Purcell, R.H. & Johnson, P.R. (1989) Nucleotide sequence analysis of feline immunodeficiency virus: genome organization and relationship to other lentiviruses. *Proc. Natl. Acad. Sci. USA* **86**, 8088-8092.

[9] Talbott, R.L., Sparger, E.E., Lovelace, K.M.,Fitch, W.M., Pedersen, N.C., Luciw, P.A. & Elder, J.H. (1989) Nucleotide sequence and genomic organization of feline immunodeficiency virus. *Proc. Natl. Acad. Sci. USA* **86**, 5743-5747.

[10] Olmsted, R.A., Barnes, A.K., Yamamoto, J.K., Hirsch,V.M., Purcell, R.H. & Johnson, P.R. (1989) Molecular cloning of feline immunodeficiency virus. *Proc. Natl. Acad. Science USA* **86**, 2448-2452.

[11] Egberink, H.F., Ederveen, J., Montelaro, R.C., Pederson, N.C., Horzinek. M.C. & Koolen, M.J.M. (1990) Intracellular proteins of feline immunodeficiency virus and their antigenic relationship with equine infectious anaemia virus proteins. *J. Gen. Virol.* **71**, 739-743.

[12] Momany, C., Kovari, L.C., Prongay, A.J., Keller, W., Gitti, R.K., Lee, B.M.,Gorbalenya, A.E., Tong, L., McClure, J., Ehrlich, L.S., Summers, M.F., Carter, C. & Rossmann, M.G. (1996) Crystal structure of dimeric HIV-1 capsid protein. *Nature Struct. Biol.* **3**, 763-770.

[13] Gitti, R.K., Lee, B.M., Walker, J., Summers, M.F., Yoo, S. & Sundquist, W.I. (1996) Structure of the amino-terminal core domain of the HIV-1 capsid protein. *Science* **273**, 231-235.

[14] Gamble, T.R., Yoo, S., Vadjos, F.F., von Schwedler, U.K., Worthylake, D.K.,Wang, H., McCutcheon, J.P., Sundquist, W.I. & Hill, C.P. (1997) Structure of the carboxyl-terminal dimerization domain of the HIV-1 capsid

protein. *Science* **278**, 849-852.

[15] Jin, Z., Jin, L., Peterson, D.L. & Lawson, C.L. (1999) Model for lentivirus capsid core assembly based on crystal dimers of EIAV p26. *J. Mol. Biol.* **286**, 83-93.

[16] Berthet-Colominas, C., Monaco, S., Novelli, A., Sibaï, G., Mallet, F. & Cusack, S. (1999) Head-to-tail dimers and interdomain flexibility revealed by the crystal structure of HIV-1 capsid protein (p24) complexed with a monoclonal antibody Fab. *EMBO J*. **18**, 1124-1136.

[17] Sambrook, J., Fritsch, E.F. & Maniatis, T. (1989) *Molecular Cloning. A Laboratory Manual*, 2nd edn. Cold Spring Harbor Laboratory, Cold Spring Harbor NY.

[18] Farabaugh, P.J. (1978) Sequence of the lacI gene. *Nature* **274**, 765-769.

[19] O'Farrell, P.H. (1975) High resolution two-dimensional electrophoresis of proteins. *J. Biol. Chem.* **250**, 4007-4021.

[20] Perczel, A., Hollósi, M., Tusnády, G. & Fasman, G.D. (1991) Convex constraint analysis: a natural deconvolution of circular dichroism curves of proteins. *Prot. Eng.* **4**, 669-679.

[21] Edelhoch, H. (1967) Spectroscopic determination of tryptophan and tyrosine in proteins. *Biochemistry* **6**, 1948-1954.

[22] Hirel, P.H., Schmitter, M.J., Dessen, P., Fayat, G. & Blanquet, S. (1989) Extent of N-terminal methionine excision from Escherichia coli proteins is governed by the side-chain length of the penultimate amino acid. *Proc. Natl. Acad. Sci. USA* **86**, 8247-8251.

[23] Woody, R.W. & Dunker, A.K. (1996) Aromatic and cystine side chain circular

dichroism in proteins. In *Circular Dichroism and the Conformational Analysis of Biomolecules* (Fasman, G. ed), pp 109-157. Plenum Press, New York.

[24] Royer, C.A., Mann, C.J. & Matthews, C.R. (1993) Resolution of the fluorescence equilibrium unfolding profile of trp aporepressor using single tryptophan mutants. *Protein Sci.* **2**, 1844-1852.

[25] Mårtensson, L.G., Jonasson, P., Freskgård, P.O., Svensson, M., Carlsson, U. & Jonsson, B.H. (1995) Contribution of individual tryptophan residues to the fluorescence spectrum of native and denatured forms of human carbonic anhydrase II. *Biochemistry* **34**, 1011-1021.

[26] Cai, K. & Schirch, V. (1996) Structural studies on folding intermediates of serine hydroxymethyltransferase using single tryptophan mutants. *J. Biol. Chem.* **271**, 2987-2994.

[27] Elyar, J.S., Tellier, M.C., Soos, J.M. & Yamamoto, J.K. (1997) Perspectives on FIV vaccine development. *Vaccine* **15**, 1437-1444.

[28] Mammano, F., O'Hagen, A., Hoglund, S. & Gottlinger, H.G. (1994) Role of the major homology region of human immunodeficiency virus type 1 in virion morphogenesis. *J. Virol.* **68**, 4927-4936.

[29] Chazal, N., Gay, B., Carrière, C., Tournier, J. & Boulanger, P. (1995) Human immunodeficiency virus type 1 MA deletion mutants expressed in baculovirus-infected cells: cis and trans effects on the Gag precursor assembly pathway. *J. Virol.* **69**, 365-375.

[30] Reicin, A.S., Paik, S., Berkowitz, R.D., Luban,J.,Lowy, I. & Goff, S.P. (1995) Linker insertion mutations in the human immunodeficiency virus type 1 gag

gene: effects on virion particle assembly, release, and infectivity. *J. Virol.* **69**, 642-650.

[31] Jarrett, O., Yamamoto, J.K. & Neil, J.C. (1990) Feline immunodeficiency virus as a model for AIDS vaccination. *AIDS* **4**, 163-165.

[32] Bennett, M. & Hart, C.A. (1995) Feline immunodeficiency virus infection-a model for HIV and AIDS? *J. Med. Microbiol.* **42**, 233-236.

[33] Ehrlich, L.S., Agresta, B.E., Gelfand, C.A., Jentoft, J. & Carter, C.A. (1994) Spectral analysis and tryptic susceptibility as probes of HIV-1 capsid protein structure. *Virology* **204**, 515-525.

[34] Hausdorf, G., Gewieß, A., Wray, V. & Porstmann, T. (1994) A recombinant human immunodeficiency virus type-1 capsid protein (rp24): its expression, purification and physico-chemical characterization. *J. Virol. Methods* **50**, 1-10.

[35] Birkett, A.J., Yélamos, B., Rodríguez-Crespo, I., Gavilanes, F. & Peterson, D.L. (1997) Cloning, expression, purification, and characterization of the major core protein (p26) from equine infectious anemia virus. *Biochim. Biophys. Acta* **1339**, 62-72.

[36] Freskgård, P.-O, Mårtensson, L.-G, Jonasson, P., Jonsson B.-H. & Carlsson, U. (1994) Assignment of the contribution of the tryptophan residues to the circular dichroism spectrum of human carbonic anhydrase II. *Biochemistry* **33**, 14281-14288.

[37] Loewenthal, R., Sancho, J. & Fersht, A.R. (1991) Fluorescence spectrum of

barnase: contributions of three tryptophan residues and a histidine-related pH dependence. *Biochemistry* **30**, 6775-6779.

[38] Wu, P. & Brand, L. (1994) Resonance energy transfer: methods and applications. *Anal. Biochem.* **218**, 1-13.

Table 1. Amino acid composition of FIV-rp24 and W40F, W126F and W40/126F mutants.

AMINO ACID	THEORETIC[a]	FIV-rp24	W40F	W126F	W40/126FF
ALA	33	32	33	32	32
ARG	11	11	11	11	11
ASX	15	16	15	16	16
CYS	4	4[b]	N.D.[c]	N.D.[c]	N.D.[c]
GLX	35	35	35	35	35
GLY	11	12	12	12	12
HIS	8	9	9	9	9
ILE	11	11	11	11	11
LEU	24	24	24	24	24
LYS	15	14	15	15	14
MET	9	8	8	8	8
PHE	7	7	8	8	9
PRO	14	15	15	15	15
SER	12	11	11	11	11
THR	11	11	11	10	10
TRP[d]	2	2	1	1	0
TYR	7	7	7	7	7
VAL	8	8	7	8	8

[a] The theoretic composition was determined from the amino acid sequence deduced from the cDNA sequence.

[b] The number of cysteine residues was determined as carboxymethylcysteine in the protein reduced and carboxyamidomethylated.

[c]N.D., not determined.

[d]The number of tryptophan residues was calculated by the method of Edelhoch [21].

Table 2. Secondary structure of FIV-rp24 and tryptophan mutants calculated from the CD spectra. The data were calculated according to the CCA method [20].

PROTEIN	α-helix(%)	β-sheet (%)	β turn (%)	Aperiodic (%)
FIV-rp24	48	0	20	32
W40F	52	0	18	30
W126F	51	0	20	29
W40/126F	49	5	14	32

LEGENDS

Fig. 1. Cloning strategy for FIV-rp24. (A) Nucleotide sequence of the primers used to amplify the p24 gene. The p24-NcoI (+) primer introduces an *Nco*I restriction site, while the p24-BglII (-) primer introduces a *Bgl*II restriction site. (B) Alignment of the original and cloned amino-terminal sequences of FIV-p24. (C) Alignment of the original and cloned carboxy-terminal sequences of FIV-p24. New restriction sites are underlined (*Nco*I- CCATGG; *Bgl*II- AGATCT) and 'TAA' is the termination codon (*) for the cloned gene.

Fig. 2. SDS-PAGE of the purification steps of the FIV-rp24 protein. Lane 1, molecular mass markers; lane 2, M15 cells without induction; lane 3, M15 cells induced with 0.25 mM IPTG for 4 h; lane 4, soluble proteins loaded onto a Ni-NTA-Agarose column; lane 5, FIV-rp24 eluted with 10 mM Tris, 200 mM Imidazol, pH 8.0.

Fig. 3. **Absorption spectra of FIV-rp24 and tryptophan mutant proteins**. FIV-rp24 (—); W40F (---); W126F (-·-) and W40/126F (·····). The protein concentration was 1 mg/ml in all cases. The buffer employed was 10 mM sodium phosphate, pH 7.0.

Fig. 4. Circular dichroism spectra of FIV-rp24 and tryptophan mutant proteins. Far-UV (A) and near-UV (B) CD spectra of FIV-rp24 (—); W40F (---); W126F (-·-) and W40/126F (·····). The protein concentration was 0.1 mg/ml (far-UV) and 1 mg/ml

(near-UV). The buffer employed was 10 mM sodium phosphate, pH 7.0. These spectra are representative of those obtained for three different preparations.

Fig. 5. **Contribution of Trp40 (A) and Trp126 (B) residues to the near-UV CD spectrum of FIV-rp24**. The contributions of each Trp was calculated by subtracting the spectrum of the corresponding single mutant from the FIV-rp24 spectrum (—) or the spectrum of the double mutant from that of the other mutant (---).

Fig. 6. **Near-UV CD spectrum of FIV-rp24 obtained by adding the contributions of tryptophan and tyrosine residues.** The experimental spectrum of FIV-rp24 (—) is compared with those obtained by adding the spectrum of double mutant and the spectra of Trp40 and Trp126. The later are obtained as indicated in Fig. 5 by subtracting from the spectrum of FIV-rp24 the spectrum of the corresponding mutant (---) or from the spectrum of the other mutant the spectrum of the double mutant (-·-).

Fig. 7. **Fluorescence emission spectra of FIV-rp24 (A) and W40F (B), W126F (C) and W40/126F (D) mutants**. Emission spectra were obtained upon excitation at 275 nm (—) and 295 nm (---). The spectra obtained upon excitation at 295 nm are normalized. The protein concentration was 0.05-0.1 mg/ml. The buffer employed was 10 mM sodium phosphate, pH 7.0. The contribution of tyrosine residues to the emission spectra of the protein (-·-) is calculated as indicated in the Experimental Procedures section. The spectra shown are representative of those obtained for three different preparations.

Fig. 8. **Thermal denaturation curves of FIV-rp24 (A), W40F (B), W126F (C) and**

W40/126F (D). The ellipticity at 208 nm was continuously monitored as the temperature was continuously increased at 30 °C/h rate. The protein concentration was 0.1-0.2 mg/ml and the buffer used was 10 mM sodium phosphate, pH 7.0. The curves shown are representative of those obtained for three different preparations.

Figure 1

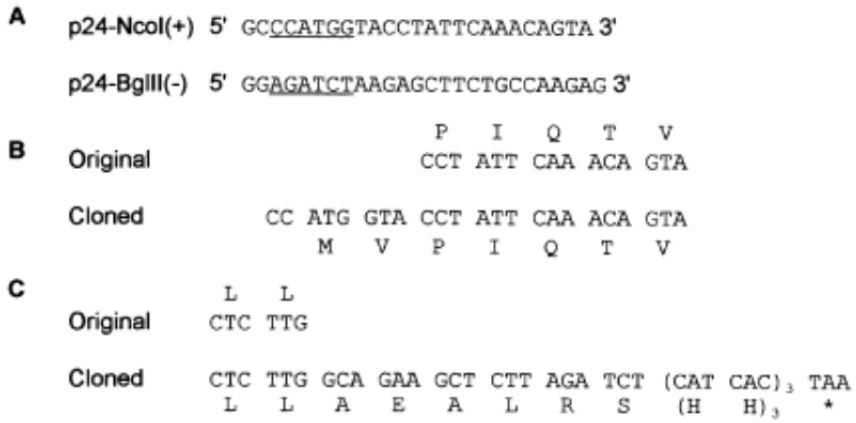

Figure 2

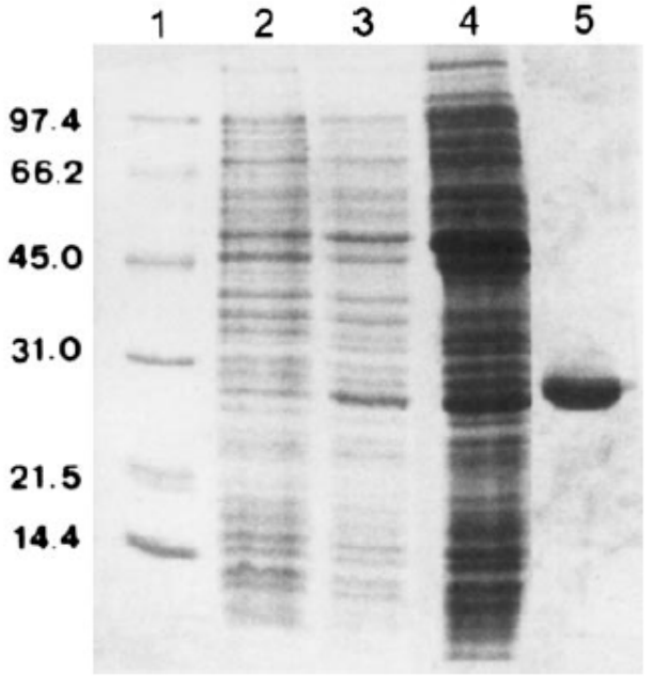

Figure3

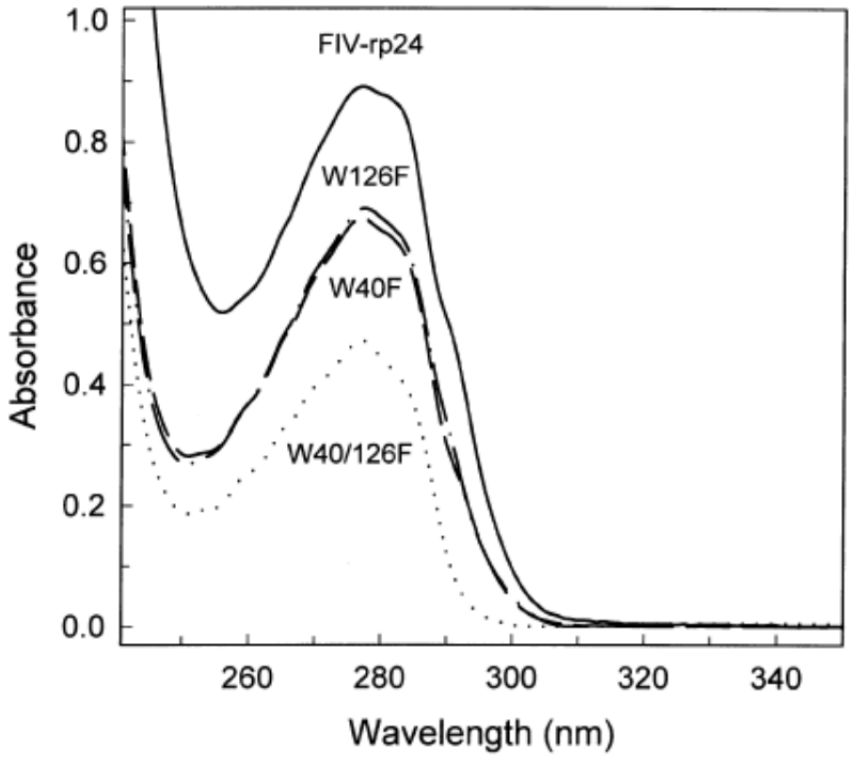

Figure 4

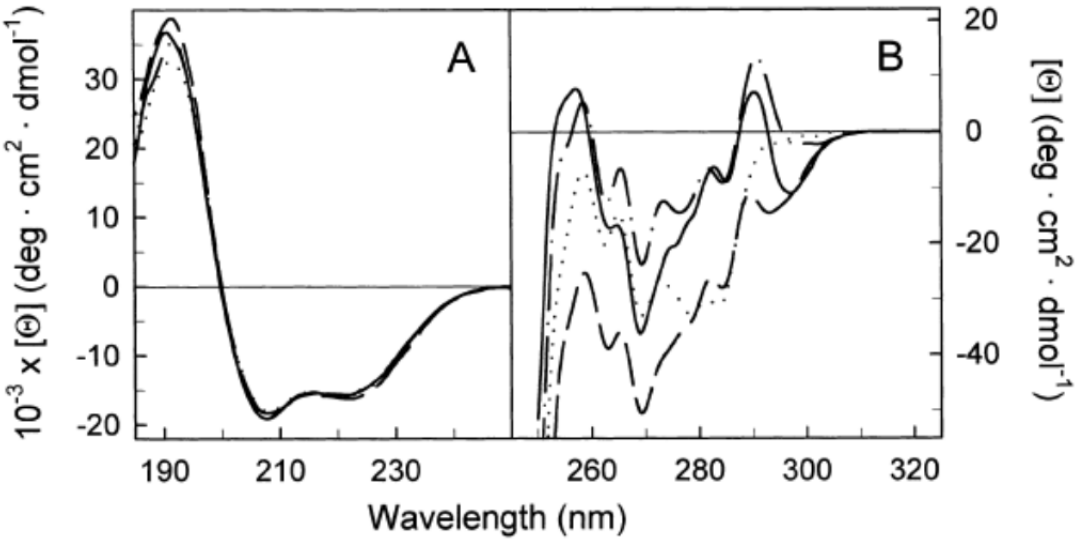

Figure 5

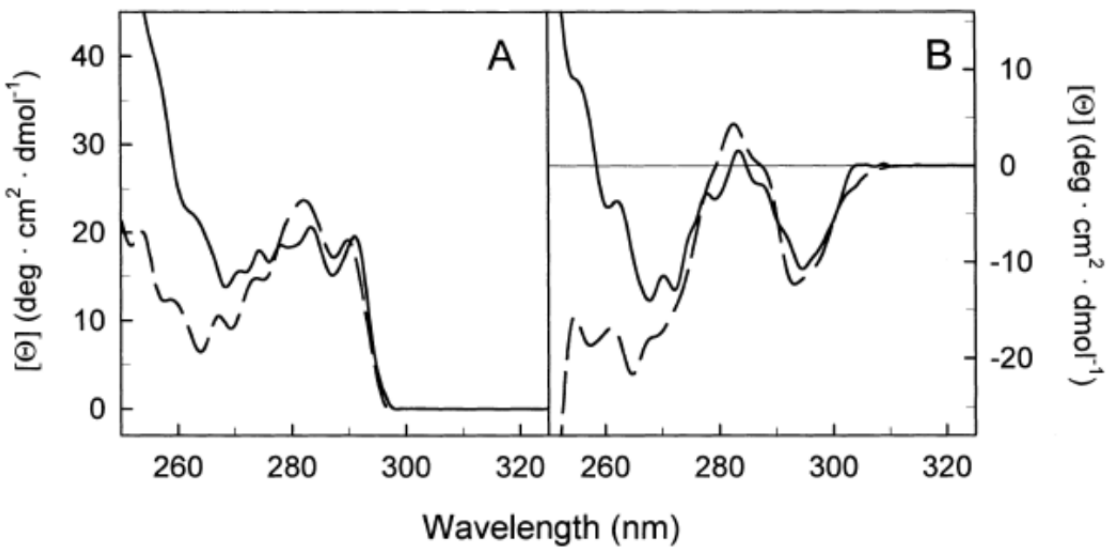

Figure 6

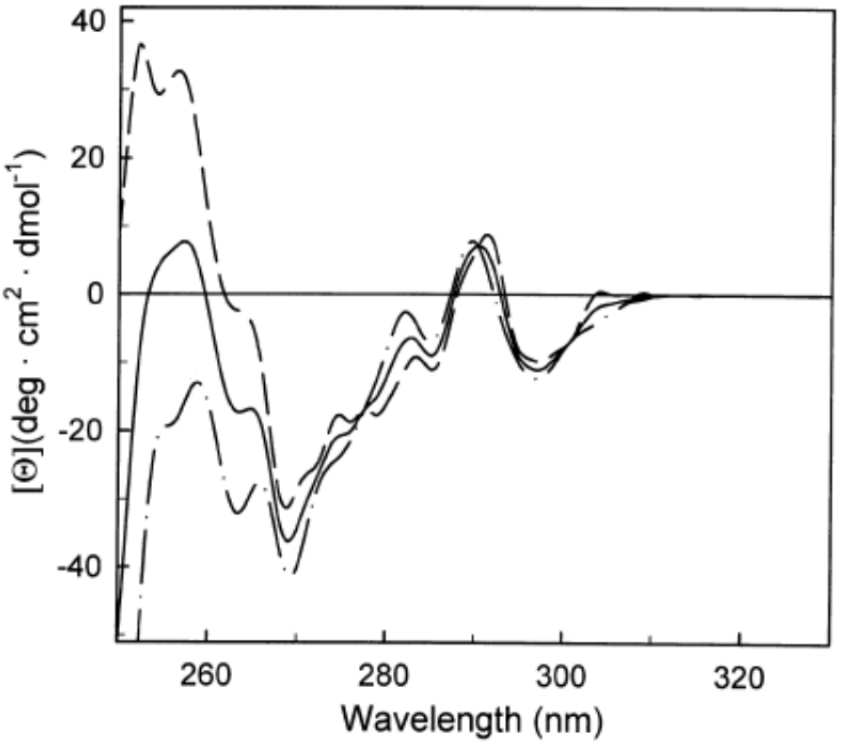

Figure 7

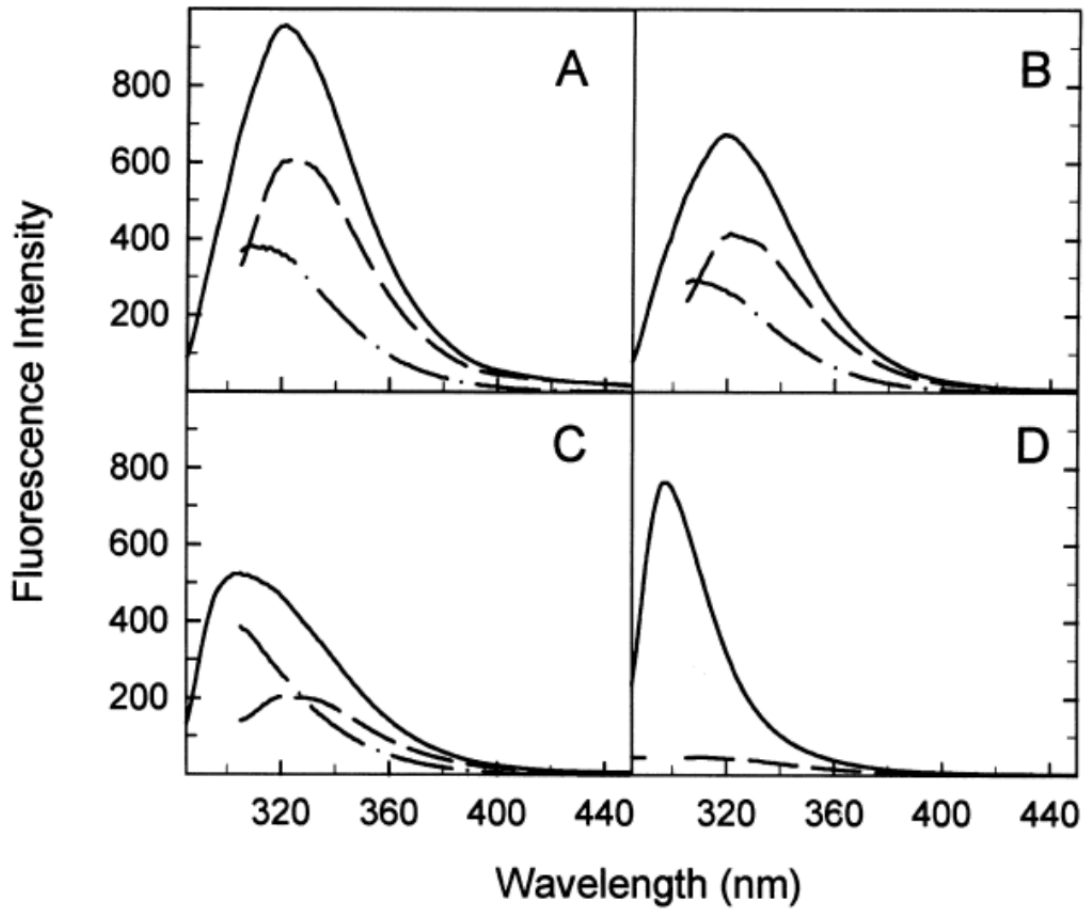
A
B
C
D
800
600
400
200
320
360
400
440
Fluorescence Intensity
Wavelength (nm)

Figure 8